

The Completed Analysis and Characteristic Investigation for Z-Shape Microstrip Antennas

¹Bo-Yuan Chang, ²Yung-Hui Shih and ^{1,*}Tung-Hung Hsieh

Abstract

This paper modifies theoretical formulation for a Z-shape microstrip antenna to obtain its resonant frequency and required parameters including the electromagnetic fields in antenna cavity, magnetic currents and radiation. Based on the comparison between theory and simulation, the distributions of electric fields along the long or short axis of the antenna structure are pretty reasonable, and the radiations of two modes remain single-beam distributed as expected. According to antenna characteristics, the length of the short axis can adjust the separation of resonant frequencies of two modes. The widths of two extension legs can also modify this frequency separation. As the ratio of these two extension legs varies, the resonant frequencies are not so affected that the whole length of the axis can be used to design for desired frequency bands. As this ratio becomes one third, the peak difference between co-polarization and cross-polarization radiations is improved effectively. As the procedure to design antennas for two specific frequency bands is followed, the mode number and the length along the long or short axis are first applied to decide resonant frequencies; the antenna characteristics are used to adjust antenna radiations later on. The theoretical effort to obtain antenna parameters here does not make formulation completed, but make antenna characteristics easier to investigate for the future design.

Keywords: dual-Band, Z-shape, microstrip antenna, theoretical analysis

1. Background and Motivation

Recently, the demand of wireless communication as well as the functions of 3C products has increased. In order to design a compact product to satisfy these applications, an antenna with

multiple-band operations becomes the trend in related research. Among those many types of antennas, the compact, co-planner microstrip antenna is the best choice because it is easy to integrate with other components on PCB. However, there is only one mode available for a conventional microstrip antenna; therefore, how to design an antenna to operate at multiple bands becomes more important than ever.

The slot H-type structure maintains the advantage of size reduction provided by the H-type microstrip antenna. The slot makes impedance easily match, and this antenna can operate at two bands [1]. There is another design which used a triangular patch to reduce an antenna size [2]. The two slots used can enhance the bandwidth for two frequency bands; however, the effect on bandwidth is so limited that the design freedom is not so good as expected.

There are many designs for the application of dual or multiple bands in the past years. For example, by cutting two small pieces at corners from a conventional microstrip, a T-shape microstrip antenna can operate at two bands [3]. Besides a concaved microstrip antenna can offer the similar feature [4]. As the microstrip patch is modified into a ladder shape, a triple-band antenna is achieved [5]. For this type of antenna, the design concept is to produce various distributions of electric fields. However, only specific dimension of an antenna can work, otherwise, radiation will be unacceptable [6]. In other word, the design concept is simple and straight, but the radiation problem is yet to solve.

In contrast, as a folded structure is applied to the T-shape microstrip antenna, radiation is improved with a thicker antenna substrate. A microstrip antenna with perfect electric conductor (PEC) walls on three sides of its own structure can also provide dual-band operation, but the freedom of two frequency bands is limited [7]. A mono-pole microstrip antenna with double-folded structure can also make original antenna operate at dual bands [8]. The design concept is to change the path of electric field in order to cancel out the currents in the opposite direction. However, less flexibility of frequency bands limits design freedom. A microstrip antenna with various disturbing patches in a substrate cavity can offer similar functions, too [9]. The antenna radiation can remain acceptable; however, the uncertainty of resonant frequencies makes antenna difficultly designed for specific bands. As a rectangular microstrip patch is reformed into a Z-shape [10], the magnetic currents on upper and lower sides are

*Corresponding Author: Tung-Hung Hsieh
(E-mail: tonyhs@isu.edu.tw)

¹ Department of Electronic Engineering, I-shou University, Kaohsiung, Taiwan 840

² Department of Materials Science and Engineering, I-shou University, Kaohsiung, Taiwan 840

transformed into the ones with the same direction on the left or right sides. Therefore, the path of electric fields horizontally or vertically determines a mode, respectively. The design is also simple, and single-beam radiation can maintain. The verification of design concept and characteristic investigation are well explained already in related research; however, the effort only focuses on the resonant frequency computation and the comparison between theoretical and simulated results. Meanwhile, the investigation is only on antennas with symmetric structure of this Z-shape so that design freedom is limited. In other word, the computation of electromagnetic waves in the cavity and the radiation in space are not completed yet. The verification of theory is insufficient so that the investigation of antenna characteristics becomes less effective. The purpose of this paper is to compensate the deficiency of the related research on the Z-shape microstrip antenna.

2. Theoretical Formulation

The structure of a Z-shape microstrip antenna is shown in Figure 1. The structure includes a microstrip patch on the upper layer, a substrate on the middle layer, and a metallic ground on the lower layer. Antenna signal is fed by a coaxial cable. The Z-shape structure is extended from a conventional rectangular patch. According to the research [11], as the resonant frequency is put back to the obtained Z-matrix, the corresponding coefficients α and β of the basis functions are obtained, and their values are based on their ratio with the resonant frequency. Later on, the magnetic field functions at both junctions of three regions $h_{12}(x)$ and $h_{23}(x)$ can be obtained after solving for the coefficients of harmonics A_{ms} 、 A_{ns} 、 B_{ns} 、 A_{ls} . Finally, the electric fields in each region are:

$$E_{z1} = -j \frac{1}{\omega \mu \epsilon} k^2 \sum_{m=0}^{Ms} A_{ms} \cdot \cos[k_{x1}(x+d)] \cdot \cos[k_{y1}(y-a-b-c)] \quad (1a)$$

$$E_{z2} = -j \frac{1}{\omega \mu \epsilon} k^2 \sum_{n=0}^{Ns} \cos[k_{x2}x] \cdot \{A_{ns} \sin[k_{y2}(y-b-c)] + B_{ns} \sin[k_{y2}(y-c)]\} \quad (1b)$$

$$E_{z3} = -j \frac{1}{\omega \mu \epsilon} k^2 \sum_{l=0}^{Ls} A_{ls} \cdot \cos[k_{x3}x] \cdot \cos[k_{y3}y] \quad (1c)$$

And the corresponding magnetic fields are:

$$H_{x1} = -\frac{1}{\mu} \sum_{m=0}^{Ms} A_{ms} \cdot k_{y1} \cdot \cos[k_{x1}(x+d)] \cdot \sin[k_{y1}(y-a-b-c)] \quad (2a)$$

$$H_{x2} = \frac{1}{\mu} \sum_{n=0}^{Ns} k_{y2} \cdot \cos[k_{x2}x] \cdot \{A_{ns} \cos[k_{y2}(y-b-c)] + B_{ns} \cos[k_{y2}(y-c)]\} \quad (2b)$$

$$H_{x3} = \frac{1}{\mu} \sum_{l=0}^{Ls} A_{ls} \cdot k_{y3} \cdot \cos[k_{x3}x] \cdot \sin[k_{y3}y] \quad (2c)$$

$$H_{y1} = -\frac{1}{\mu} \sum_{m=0}^{Ms} A_{ms} \cdot k_{x1} \cdot \sin[k_{x1}(x+d)] \cdot \cos[k_{y1}(y-a-b-c)] \quad (3a)$$

$$H_{y2} = \frac{1}{\mu} \sum_{n=0}^{Ns} k_{x2} \cdot \sin[k_{x2}x] \cdot \{A_{ns} \sin[k_{y2}(y-b-c)] + B_{ns} \sin[k_{y2}(y-c)]\} \quad (3b)$$

$$H_{y3} = \frac{1}{\mu} \sum_{l=0}^{Ls} A_{ls} \cdot k_{x3} \cdot \sin[k_{x3}x] \cdot \cos[k_{y3}y] \quad (3c)$$

According to electromagnetic theory [12], an electric field on a perfect magnetic conductor (PMC) wall of a cavity will produce a magnetic current. Meanwhile, this magnetic current can also produce its own image by applying the image theory. Therefore, the strength of a final magnetic current M will double due to an infinite ground:

$$\vec{M} = -2\hat{n} \times \vec{E}_z \quad (4)$$

Where \hat{n} represents a unit vector along the normal direction on a PMC wall, and \vec{E}_z is the electric field of a particular mode at the same wall. Therefore, for this Z-shape microstrip antenna, the magnetic currents transformed from the electric fields at individual region are demonstrated in Figure 2, i.e.:

$$\vec{M}_1 = 2 \sum_{m=0}^{Ms} A_{ms} \cdot \cos[ms \cdot \pi] \cdot \cos[k_{y1}(y-a-b-c)] \cdot \hat{a}_y \quad (5a)$$

$$\vec{M}_2 = 2 \sum_{n=0}^{Ns} A_{ns} \cdot \cos[k_{x1}(x+d)] \cdot \sin[k_{y1}a] \cdot \hat{a}_x \quad (5b)$$

$$\vec{M}_3 = 2 \sum_{n=0}^{Ns} A_{ns} \cdot \cos[ns \cdot \pi] \cdot \{A_{ns} \cdot \cos[k_{y2}(y-b-c)] + B_{ns} \cdot \cos[k_{y2}(y-c)]\} \cdot \hat{a}_y \quad (5c)$$

$$\vec{M}_4 = 2 \sum_{l=0}^{Ls} A_{ls} \cdot \cos[ls \cdot \pi] \cdot \cos[k_{y3}y] \cdot \hat{a}_y \quad (5d)$$

$$\vec{M}_5 = 2 \sum_{b=0}^{L_s} A_b \cdot \cos[k_{x3}x] \cdot \hat{a}_x \quad (5e)$$

$$\vec{M}_6 = 2 \sum_{b=0}^{L_s} A_b \cdot \cos[k_{y3}y] \cdot \hat{a}_y \quad (5f)$$

$$\vec{M}_7 = 2 \sum_{b=0}^{L_s} A_b \cdot \sin[k_{y3}c] \cdot \cos[k_{x3}x] \cdot \hat{a}_x \quad (5g)$$

$$\vec{M}_8 = 2 \sum_{ns=0}^{N_s} A_{ns} \cdot \{A_{ns} \cdot \cos[k_{y2}(y-b-c)] + B_{ns} \cdot \cos[k_{y2}(y-c)]\} \cdot \hat{a}_y \quad (5h)$$

$$\vec{M}_9 = 2 \sum_{ms=0}^{M_s} A_{ms} \cdot \cos[k_{y1}(y-a-b-c)] \cdot \hat{a}_y \quad (5i)$$

$$\vec{M}_{10} = 2 \sum_{ms=0}^{M_s} A_{ms} \cdot \cos[k_{x1}(x+d)] \cdot \hat{a}_x \quad (5j)$$

where \vec{M}_1 、 \vec{M}_3 、 \vec{M}_4 、 \vec{M}_6 、 \vec{M}_8 、 \vec{M}_9 are the magnetic currents along \hat{x} direction, and \vec{M}_2 、 \vec{M}_5 、 \vec{M}_7 、 \vec{M}_{10} are those along \hat{y} direction. According to the concept of radiation computation from a magnetic current, the radiation in open space can be divided into the vector electric potential \vec{F}_x in \hat{x} direction, and \vec{F}_y in \hat{y} direction:

$$\vec{F}_x = \frac{\varepsilon e^{-jkr}}{4\pi r} \iint_s (\vec{M}_2 + \vec{M}_5 + \vec{M}_7 + \vec{M}_{10}) e^{jk_y r' \cos\phi} ds' \quad (6a)$$

$$\vec{F}_y = \frac{\varepsilon e^{-jkr}}{4\pi r} \iint_s (\vec{M}_1 + \vec{M}_3 + \vec{M}_4 + \vec{M}_6 + \vec{M}_8 + \vec{M}_9) e^{jk_y r' \cos\phi} ds' \quad (6b)$$

where the notation s' for integration is the area on an individual PMC wall where a magnetic current exists. And, r and r' represent the distances between observation point and magnetic current source or the origin. Meanwhile, the phase difference is rearranged as:

$$r' \cos\phi = x' \cdot \sin\theta \cos\phi + y' \cdot \sin\theta \sin\phi + z' \cdot \cos\theta \quad (7)$$

Finally, the radiating electric fields at far field are obtained:

$$E_r \approx 0 \quad (8a)$$

$$E_\theta = -jk_0(-F_x \sin\phi + F_y \cos\phi) \quad (8b)$$

$$E_\phi = jk_0(F_x \cos\theta \cos\phi + F_y \cos\theta \sin\phi) \quad (8c)$$

3. Results and Comparisons

The investigation for antenna characteristics is based on theoretical data because the verification has been done in [13]. The paths to investigate the electric fields in the antenna cavity of this Z-shape antenna include three different ones, near or along the long axis for lower or higher modes, which are indicated in Figures 3 and 4.

The field is continuous at all the junctions of three regions indicated in Figure 5. The observation verifies the theoretical computation as compared with the design scheme. For the lower mode, the electric fields along the three paths are shown in Figure 6. The distribution of the fields all maintains cosine curve since the PMC boundaries of the cavity are well defined. However, it is also reasonable that the amplitudes of electric fields are different from each other, which is due to the PMC boundary on the upper side of this cavity. The distributions of electric fields in region II are also shown in Figure 7, and they are all reasonable as expected. Besides, the distribution of the field in region III is the same as that in region I as shown in Figure 8, because the structure is anti-symmetric along the horizontal axis.

Since the path to determine the higher mode is in region II, the discussion of this section only focuses on the field along the short path in region II as indicated Figure 9. Notice that those fields are also cosine distributed along three paths due to the PMC boundaries on the left and right sides of the cavity. The distributions of electric fields in region I and II are shown in Figures 10 and 11. The result confirms the fact that these distributions are extended from that in region II.

Figure 12 shows that the resonant frequency of higher mode increases as the length along the horizontal axis decreases. Meanwhile, the resonant frequency of lower mode remains unchanged because the whole length of long axis does not vary too much. The fact reveals that the separation between two frequency bands is able to change by the length of long axis

As the widths of two legs are adjusted, the results are demonstrated in Figure 13. As the leg gets narrower, the resonant frequency of low mode increases, while the higher one decreases. This is expected because the cavity becomes smaller as the leg becomes narrower. As the leg width gets narrower and narrower, the structure turns to be the same as a rectangular one. As a result of fact, the resonant frequency of higher mode is close to the 2.7 GHz of a rectangular microstrip antenna.

The result in Figure 14 shows that the resonant frequency of lower mode increases since the cavity becomes smaller as a single leg gets narrower. However, the one of the higher mode decreases because of the less influence of structure bending. Although the result is similar as legs changes together, the variation of resonant frequency is not so significant that it is not a good idea to use the leg width to control resonant frequencies.

When the lengths of two legs are different from each other, and the whole dimension of antenna is fixed, the variation of resonant frequency vs. leg length (d and f) is shown in Figure 15. The value of resonant frequency is not affected as the ratio of legs changes since the whole path length for lower mode does not change, either. The similar situation happens to the higher mode. In other word, the value of this value is the good choice to set up frequency bands in design at first. Besides, the peak difference of co-polarization and cross-polarization radiation on E-plane are between the values of 18 to 28 dB as shown in Figure 16. This is well acceptable because the situation is the same as that on H-plane. In other word, the radiation of higher mode is not affected too much, so it is not necessary to consider the radiation problem for this mode in design.

The peak difference of radiation on E-plane for higher mode as leg length changes is demonstrated in Figure 17. As the ratio of lengths between two legs is within the range from 0.2 to 0.4, the peak difference between co-polarization and cross-polarization radiation is about 12dB, which is well acceptable. As the ratio approaches one, this difference decreases. The trend of peak difference on H-plane is similar to that on E-plane except that the value is only about 8dB. The problem can be improved by the method discussed earlier.

The design of a Z-shape microstrip antenna for specific frequency bands is also provided here. According to the investigation earlier, the two resonant frequencies are determined by the long and short paths of Z-shape structure, so these two paths are used to adjust these resonant frequencies. While the extension legs can affect magnetic currents, they are used to modify antenna radiation. In this section, the antenna is designed at commercial bands such as 900MHz、1800MHz, and 1800MHz、2600MHz, respectively. The simulated resonant frequencies of the antenna with specific dimensions are listed in Tables 1 and 2. For the set of 900MHz and 1800MHz, the obtained data only has the errors of about 2.6 and 1.7%. For the set of 1800MHz and 2600MHz, the errors are 4.2 and 1.5%. Both cases show that expected frequency bands are achieved. However, the radiation of lower mode for the first set is not acceptable yet since cross-polarization radiation is too high. After adjustment, the radiation becomes acceptable as shown in Figures 18 and 19. Good radiation for the second set is also demonstrated in Figures 20 and 21.

4. Conclusions

For a Z-shape microstrip antenna, this paper first modifies formulations to solve for its resonant frequency and undetermined coefficient. Then electromagnetic fields in the antenna cavity, magnetic currents and radiation are obtained. Theoretical results prove that the electric field distribution along the long axis of antenna structures agrees with that of cosine function, but the distribution is more dramatic than that of an antenna without extension. In practice, the mode number along the long or short axis is the one to decide the resonant frequency of antenna. Both radiation results from theory and simulation agree with each other, and they are all acceptable. According to investigation, the extension legs of this Z-shape structure do not affect radiation too much, and the length of short path can adjust the separation of two resonant frequencies in addition to the length ratio of two legs. The optima radiation occurs when the ratio is about 1 to 3. A Z-shape antenna is also designed at two different sets of specific bands to demonstrate the design freedom of antennas.

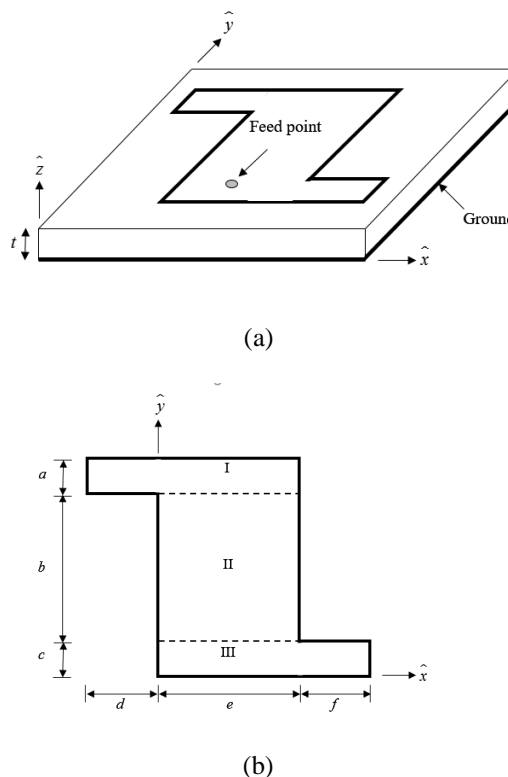


Figure 1: The structure of a Z-shape microstrip: (a) 3-D view, (b) top view.

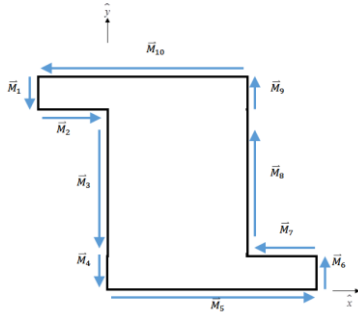


Figure 2: The magnetic currents of the Z-shape microstrip antenna in Figure 1.

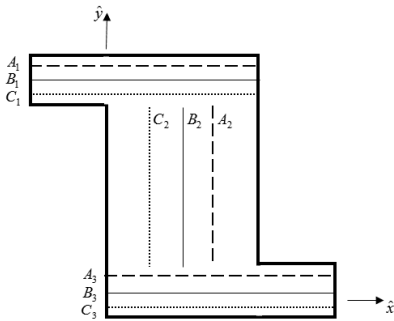


Figure 3: For the Z-shape microstrip antenna in Figure 1, three different paths used to observe the electric field distribution of the lower mode: dash line for path A, solid line for path B, dot line for path C, respectively.

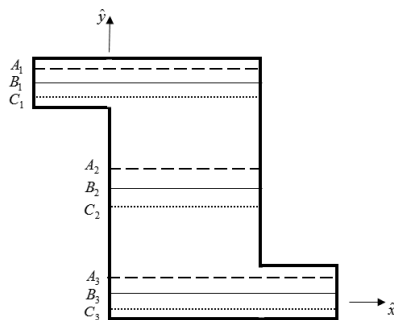


Figure 4: For the Z-shape microstrip antenna in Figure 1, three different paths used to observe the electric field distribution of the lower mode: dash line for path A, solid line for path B, dot line for path C, respectively.

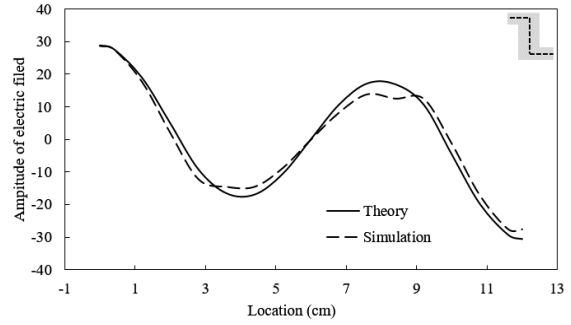


Figure 5: For the lower mode of the antenna in Figure 2, the theoretical and simulated electric fields along long path B. The structure dimensions of the antenna are: $a = 1\text{cm}$, $b = 5\text{cm}$, $c = 1\text{cm}$, $d = 2\text{cm}$, $e = 2\text{cm}$, $f = 2\text{cm}$, $t = 20\text{mils}$, $\epsilon_r = 3.35$.

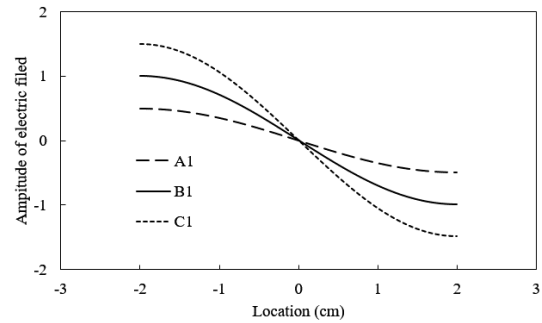


Figure 6: For the lower mode of the antenna in Figure 3, the theoretical distribution of electric fields in region I along three different paths. The structure dimensions of the antenna are: $a = 1\text{cm}$, $b = 5\text{cm}$, $c = 1\text{cm}$, $d = 2\text{cm}$, $e = 2\text{cm}$, $f = 2\text{cm}$, $t = 20\text{mils}$, $\epsilon_r = 3.35$.

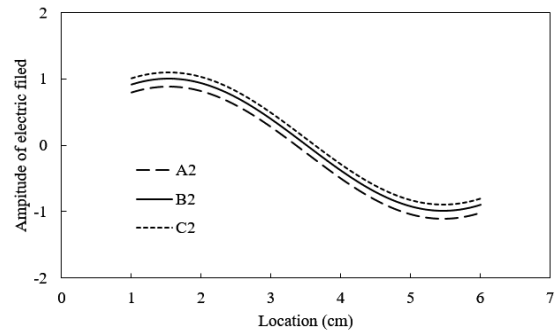


Figure 7: For the lower mode of the antenna in Figure 3, the theoretical distribution of electric fields in region II along three different paths. The structure dimensions of antennas are as those in Figure 5.

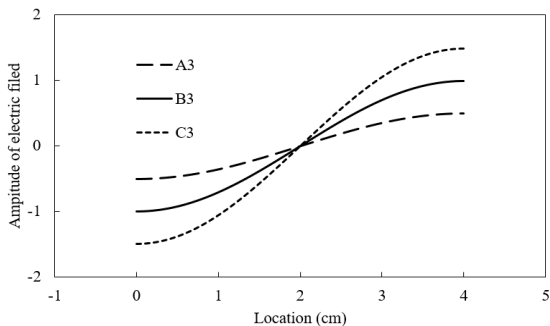


Figure 8: For the lower mode of the antenna in Figure 3, the theoretical distribution of electric fields in region III along three different paths. The structure dimensions of antennas are as those in Figure 5.

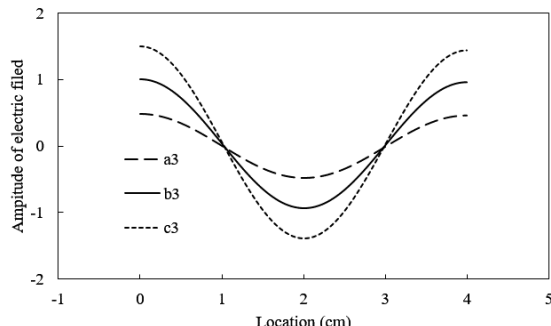


Figure 11: For the higher mode of the antenna in Figure 4, the theoretical distribution of electric fields in region III along three different paths. The structure dimensions of antennas are as those in Figure 5.

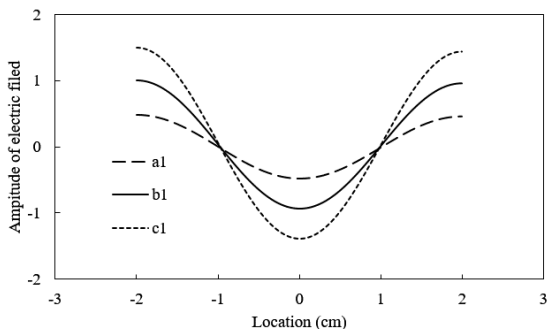


Figure 9: For the higher mode of the antenna in Figure 4, the theoretical distribution of electric fields in region I along three different paths. The structure dimensions of antennas are as those in Figure 5.

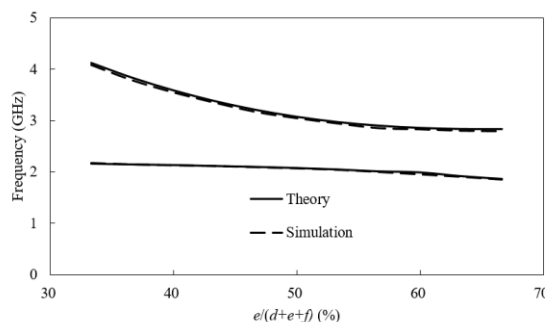


Figure 12: For the Z-shape microstrip antenna in Figure 1, the theoretic and simulated resonant frequency vs. the length of short path. The structure dimensions of the antenna are: $a=1\text{cm}$, $b=4\text{cm}$, $c=1\text{cm}$, $t=20\text{mils}$, $\epsilon_r = 3.35$.

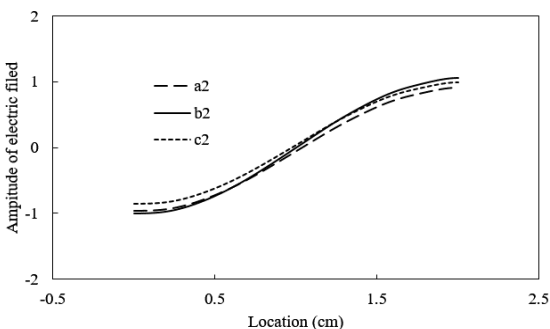


Figure 10: For the higher mode of the antenna in Figure 4, the theoretical distribution of electric fields in region II along three different paths. The structure dimensions of antennas are as those in Figure 5.

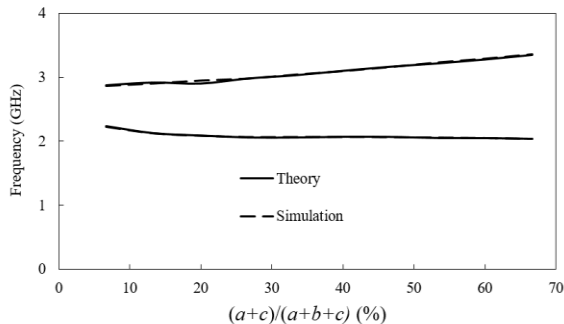


Figure 13: For the Z-shape microstrip antenna in Figure 1, the theoretic and simulated resonant frequency vs. the length of long path. The structure dimensions of the antenna are: $d = 1.5\text{cm}$, $e = 3\text{cm}$, $f = 1.5\text{cm}$, $t = 20\text{mils}$, $\epsilon_r = 3.35$.

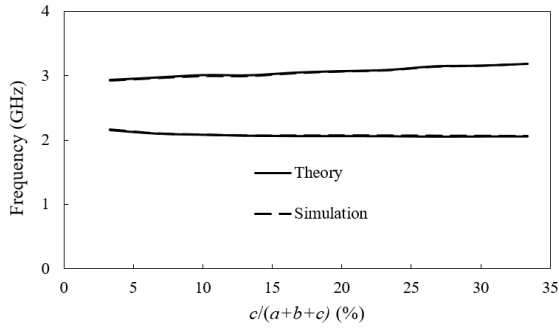


Figure 14: For the Z-shape microstrip antenna in Figure 1, the theoretical and simulated resonant frequency vs. the width of an individual leg. The structure dimensions of the antenna are: $a=1\text{cm}$, $d=1.5\text{cm}$, $e=3\text{cm}$, $f=1.5\text{cm}$, $t=20\text{mils}$, $\epsilon_r = 3.35$.

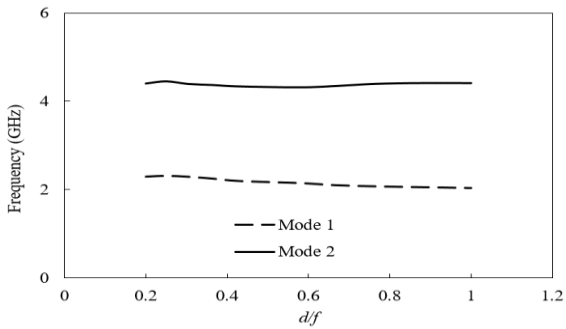


Figure 15: For the Z-shape microstrip antenna in Figure 1, the theoretical and simulated resonant frequency vs. the length ratio of two legs. The structure dimensions of the antenna are: $a = 1\text{cm}$, $b = 3\text{cm}$, $c = 1\text{cm}$, $d + f = 6\text{cm}$, $t = 20\text{mils}$, $\epsilon_r = 3.35$.

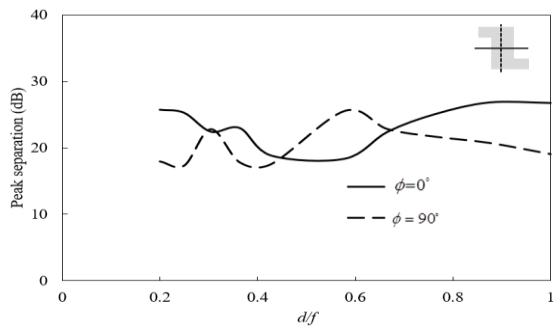


Figure 16: For the higher mode of the Z-shape microstrip antenna in Figure 1, peak difference of radiation strength vs. the length ratio of two legs in antenna structure: solid line for horizontal plane, dash line for vertical plane. The structure dimensions of the antenna are as those in Figure 15.

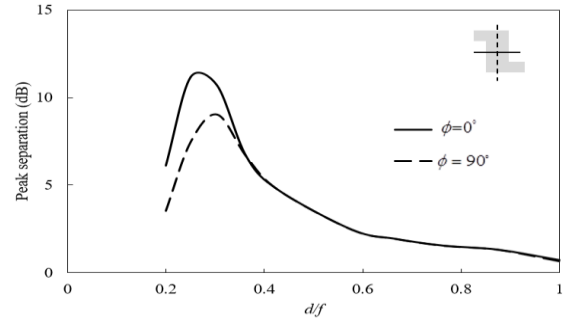


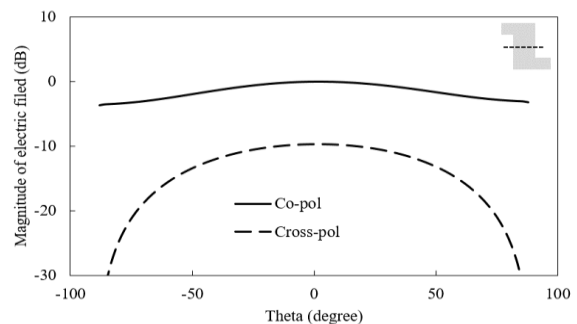
Figure 17: For the lower mode of the Z-shape microstrip antenna in Figure 1, peak difference of radiation strength vs. the length ratio of two legs in antenna structure: solid line for horizontal plane, dash line for vertical plane. The structure dimensions of the antenna are as those in Figure 15.

Table 1: For the Z-shape microstrip antenna in Figure 1, simulated resonant frequencies of two desired modes. The structure dimensions of the antenna are: $a = 1\text{cm}$, $b = 16\text{cm}$, $c = 0.1\text{cm}$, $d = 3\text{cm}$, $e = 4.5\text{cm}$, $f = 3\text{cm}$, $t = 20\text{mils}$, $\epsilon_r = 3.35$, feeding at $(0.3, 8.1)$.

	Frequency band(MHz)	theory(MHz)	error
Lower mode	900	876	2.6%
High mode	1800	1831	1.7%

Table 2: For the Z-shape microstrip antenna in Figure 1, simulated resonant frequencies of two desired modes. The structure dimensions of the antenna are: $a = 1\text{cm}$, $b = 6\text{cm}$, $c = 0.1\text{cm}$, $d = 2\text{cm}$, $e = 3.2\text{cm}$, $f = 2\text{cm}$, $t = 20\text{mils}$, $\epsilon_r = 3.35$, feeding at $(0.3, 3.1)$

	Frequency band (MHz)	theory (MHz)	error
Lower mode	1800	1877	4.2%
High mode	2600	2641	1.5%



(a)

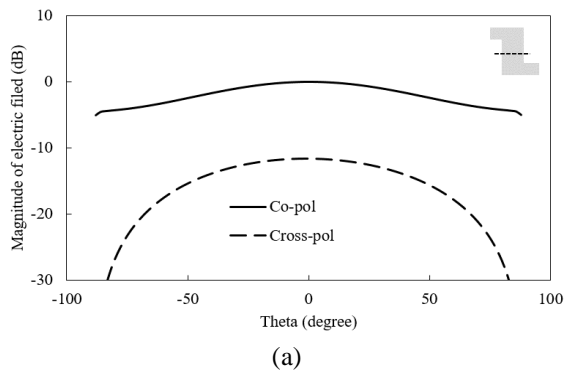
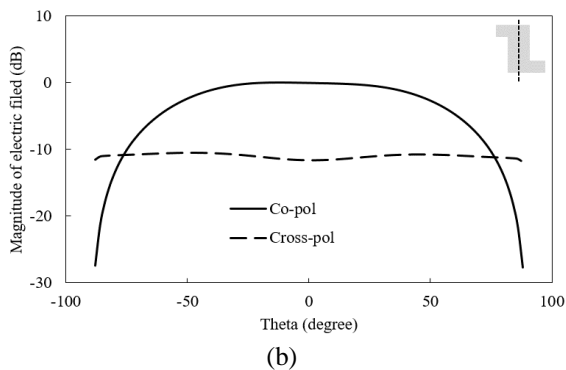


Figure 18: For the lower mode of the Z-shape microstrip antenna in Figure 1, the theoretical radiation patterns on two different planes: (a) $\phi = 0^\circ$, (b) $\phi = 90^\circ$. The structure dimensions of antennas are those in Table 1.

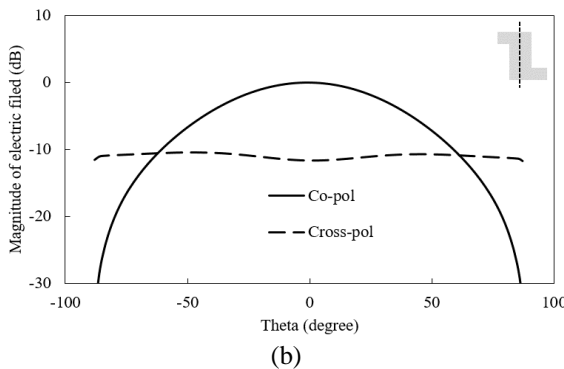
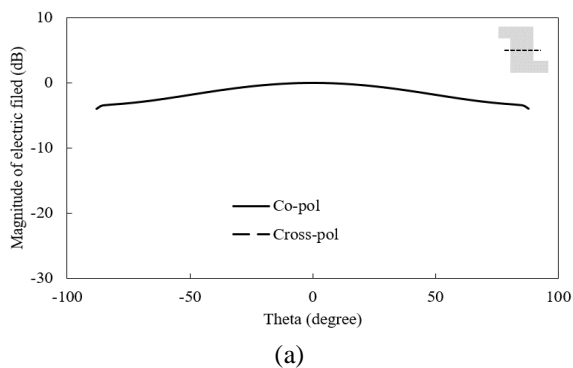


Figure 20: For the lower mode of the Z-shape microstrip antenna in Figure 1, the theoretical radiation patterns on two different planes: (a) $\phi = 0^\circ$, (b) $\phi = 90^\circ$. The structure dimensions of antennas are as those in Table 2.

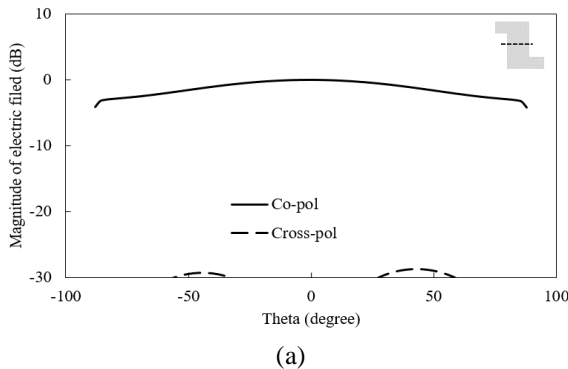
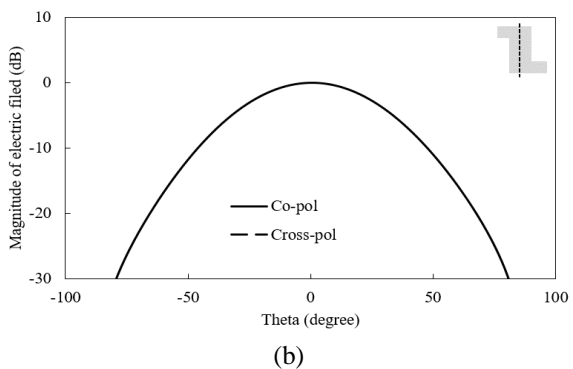


Figure 19: For the higher mode of the Z-shape microstrip antenna in Figure 1, the theoretical radiation patterns on two different planes: (a) $\phi = 0^\circ$, (b) $\phi = 90^\circ$. The structure dimensions of antennas are as those in Table 1.

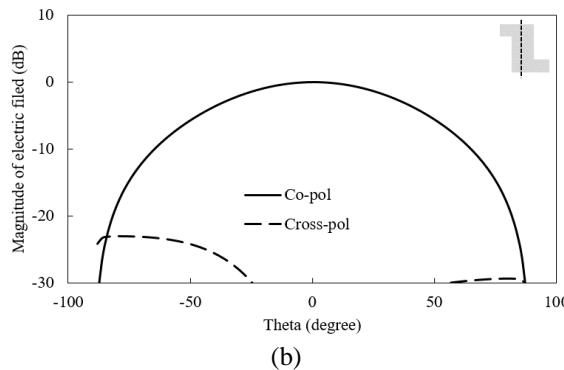


Figure 21: For the higher mode of the Z-shape microstrip antenna in Figure 1, the theoretical radiation patterns on two different planes: (a) $\phi = 0^\circ$, (b) $\phi = 90^\circ$. The structure dimensions of antennas are as those in Table 2.

References

- [1]. S. Panusa, M. Kumar, "Dual-band H-slot microstrip patch antenna for WLAN application," 2014 International Conference on Medical Imaging, m-Health and Emerging Communication Systems (Med Com), pp. 20-23, Nov. 2014.
- [2]. A. A. Deshmukh, S. Nagarbowdi, and N. V. Phatak, "Analysis of shorted V-slot cut dual and wide band triangular microstrip antenna," 2015 Communication, Information & Computing Technology (ICCICT), pp. 1-6, Jan. 2015.
- [3]. C.-L. Tai, T.-H. Hsieh, H.-T. Cheng, "T-shape Microstrip Antenna for Dual-Band Operation," 2009 National Symposium on Telecommunication, pp. 193, National University of Kaohsiung, Taiwan, 2009.
- [4]. H. Nakano and K. Vichien, "Dual-Frequency Square Patch Antenna with Rectangular Notch," Electronics Letters, Vol.25, no. 16, pp.1067-1068, Aug. 1989.
- [5]. H.-T. Cheng, Ladder-Shape Microstrip Antenna for Triple-Band Operation, Master thesis, I-Shou University, Kaohsiung, Taiwan, 2012.
- [6]. T.-H. Hsieh, C.-L. Tai, G.-C. Wang, "T-Shape Microstrip Antenna for Dual-Band Operation", International Journal of Computer; Consumer and Control (IJ3C), Vol. 3, No. 3. pp. 21-31, 2014.08
- [7]. C. S. Lee, and V. Nalbandian, "Dual-band microstrip antenna with and airgap," IEEE Antenna and Propagation Society International Symposium, Vol. 1, pp. 479-482, Jul. 1992.
- [8]. C.-C. Lin, Double-Folded Monopole Microstrip Antenna for Dual-Band Operation, Master thesis, I-Shou University, Kaohsiung, Taiwan, 2015
- [9]. Y.-H. Shih, K.-N. Huang, C.-C. Lin, C.-C. Chen, T. H. Hsieh, "The Design of Dual or Multi-Band Microstrip Antennas by Using Disturbing Patches", International Journal of Computer; Consumer and Control (IJ3C), Vol. 3, No. 4. pp. 46-57, 2014.11
- [10]. Y.-M. Cheng, Z-Shape Microstrip Antenna for Dual-Band Operation, Master thesis, I-Shou University, Kaohsiung, Taiwan, 2013.
- [11]. T.-H. Hsieh, Y.-M. Cheng, G.-C. Wang, P.-W. Chen, "The analysis of Z-shape microstrip antenna for dual-band operation", 2014 international symposium on computer, consumer and control, pp.852-855, Taichung, Taiwan, 2014.06.
- [12]. Robert S. Elliott, Antenna Theory Analysis and Design, Revised Edition, 2000.
- [13]. B.-Y. Chang, The Completed Analysis and Characteristic Investigation for Z-shape Microstrip Antenna, Master thesis, I-Shou University, Kaohsiung, Taiwan, 2016.



Bo-Yuan Chang was born in Yunlin, Taiwan, in 1993. He received the B.S. degree in Electronic Engineering from the I-Shou University in 2015. He is currently pursuing the M.S. degree in Electronic Engineering at I-Shou University, Kaohsiung, Taiwan.



Yung-Hui Shih was born in Taipei, Taiwan in 1964. He received the bachelor degree in Physics and the master degree in Materials Science and Engineering, both from the National Tsing Hua University, Taiwan, in 1986 and 1988, respectively. In 1993, he received the Ph. D. degree in Materials Science and Engineering from the North Carolina State University, Raleigh, NC, USA. His research work involved the electromagnetic properties of materials. Since 1993, he joined the I-Shou University, Kaohsiung, Taiwan, and was an associated professor of Materials Science and Engineering. His main interest of research is in the field of microstrip antenna analysis.



Tung-Hung Hsieh received the B.S. degree in Engineering Science from National Cheng Kung University, Tainan, Taiwan in 1987, the M.S. degree in Electrical Engineering from Washington University, St. Louis, Missouri, in 1990, and the Ph.D. degree in Electrical Engineering from Southern Methodist University, Dallas, Texas in 1998. In 2000 and 2001, he worked in the OSE, Kaohsiung, Taiwan, and USI, Nantou, Taiwan, respectively. Dr Hsieh is currently an Assistant Professor in the Department of Electronic Engineering at I-Shou University, Kaohsiung, Taiwan. His research interests include computational electromagnetics and design of microstrip antennas.